

# Computational Study of Carbostannylation Implicating Bimetallic Catalysis Involving “Au<sup>I</sup>–Vinyl–Pd<sup>II</sup>” Species

Alireza Ariafard,<sup>\*,†,‡</sup> Nasir Ahmad Rajabi,<sup>‡</sup> Mona Jalali Atashgah,<sup>‡</sup> Allan J. Canty,<sup>†</sup> and Brian F. Yates<sup>\*,†</sup>

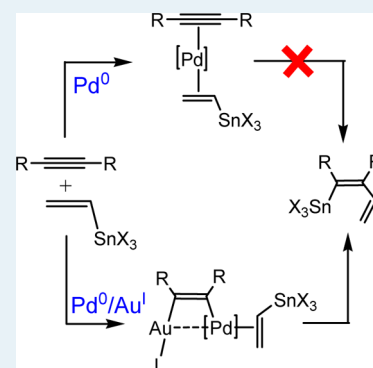
<sup>†</sup>School of Chemistry, University of Tasmania, Private Bag 75, Hobart TAS 7001, Australia

<sup>‡</sup>Department of Chemistry, Faculty of Science, Central Tehran Branch, Islamic Azad University, Shahrak Gharb, Tehran, Iran

## S Supporting Information

**ABSTRACT:** We have investigated computationally the gold and palladium cocatalyzed reaction of alkynes with vinylstannane. Our work has involved a careful and thorough exploration of different mechanistic possibilities. We find that palladium acting alone as a catalyst leads to a very high reaction barrier, consistent with the experimental observation that there is no reaction in the presence of just palladium. However, the involvement of a gold(I) complex lowers the reaction barrier considerably, and the vinylstannylation reaction can proceed with a modest activation energy of about 10 kcal/mol. Our key finding is that the introduction of the gold complex avoids the formation of high-energy structures involving vinyl species in a trans arrangement on palladium. Our work confirms the role of intermediates containing both palladium and gold as suggested by Blum. For the gold–palladium cocatalyzed reaction, we also investigated an alternative mechanism suggested by Blum. With some modifications, this mechanism has a slightly higher reaction barrier, but if it does occur, then we predict a strong dependency on the counterion, in agreement with related experimental findings.

**KEYWORDS:** bimetallic catalysis, palladium, gold, density functional theory (DFT), vinylstannylation, reaction mechanism



## INTRODUCTION

Palladium(0) complexes play a prominent role as precatalysts for coupling reactions. Although these complexes have proved to be powerful, limitations in chemical synthesis have led to the development of nontraditional methods such as bimetallic catalysis.<sup>1,2</sup> An important contemporary example of a limitation is the inability of Pd<sup>0</sup> catalysts in carbostannylation of alkynes.<sup>3</sup> In recent reports, Blum and co-workers demonstrated that Pd<sup>0</sup> alone as a catalyst does not initiate the carbostannylation reaction, whereas a combination of Pd<sup>0</sup> and Au<sup>I</sup> readily catalyzes the reaction even under mild conditions (Scheme 1).<sup>4</sup>

Blum and co-workers have provided major insights into the mechanistic detail from experimental studies and proposed two different mechanisms for the reaction. First, the reaction was proposed (Scheme 2) to proceed through intermediate I in which Pd and Au are simultaneously coordinated to the alkyne.<sup>4,5</sup> This mode of coordination is believed to enhance the  $\sigma$ -bond character of the Pd–C bonds and makes intermediate I ready for transmetalation with a vinylstannane, through transfer of the vinyl group onto the palladium and the tin group onto the nascent olefin (formation of II). Finally, the C–C reductive elimination from III leads to formation of the final product and regeneration of the Au<sup>I</sup> and Pd<sup>0</sup> catalysts.

Following this, as part of a comprehensive assessment of the field, an alternative mechanism was considered in which the carbostannylation reaction proceeds via four distinct steps (Scheme 3):<sup>2b</sup> (A) insertion of alkyne into the Pd<sup>II</sup>–C bond of IV to afford V; (B) transmetalation of the vinyl group from vinylstannane to Au<sup>I</sup> to generate intermediates VI and VII; (C)

vinyl ligand exchange between V and VI to lead to formation of IV and VIII; and (D) transmetalation of the vinyl group from vinylgold intermediate VIII to the cationic tin intermediate VII to give the final product.

Given the emerging role of bimetallic catalysts in chemistry, mechanism elucidation for this reaction may assist in designing future reaction protocols. To this end, we computationally evaluated different possible mechanisms for the carbostannylation reaction including those discussed above, and we determined which mechanism is energetically more favorable. This study demonstrates that a palladium gold vinyl intermediate is the potential active catalyst for the catalytic reaction, broadly consistent with and elaborating Blum's proposal.

## COMPUTATIONAL DETAILS

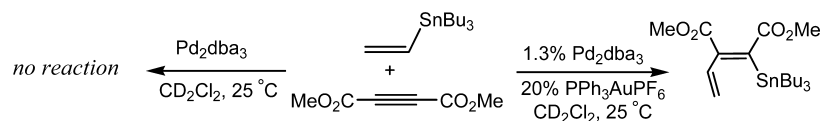
Gaussian 09<sup>6</sup> was used to fully optimize all the structures reported in this paper at the B3LYP level of density functional theory (DFT).<sup>7</sup> The effective-core potential of Hay and Wadt with a double- $\xi$  valence basis set (LANL2DZ)<sup>8</sup> was chosen to describe Au, Pd, and Sn. The 6-31G(d) basis set was used for other atoms.<sup>9</sup> Polarization functions were also added for Sn ( $\xi_d = 0.180$ ), Au ( $\xi_f = 1.050$ ), and Pd ( $\xi_f = 1.472$ ).<sup>10</sup> This basis set combination will be referred to as BS1. Frequency calculations were carried out at the same level of theory as those for the structural optimization. Transition structures were located using the Bery algorithm. Intrinsic reaction coordinate (IRC)<sup>11</sup> calculations were used to confirm the connectivity between transition structures and

Received: September 20, 2013

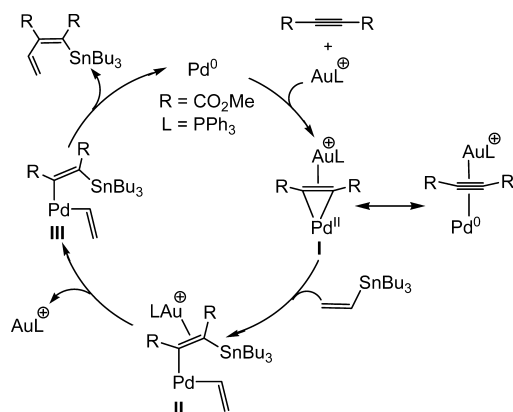
Revised: January 29, 2014

Published: February 12, 2014

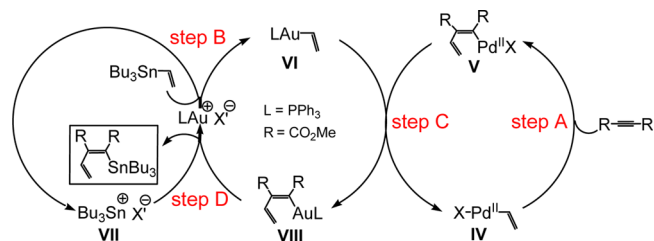
Scheme 1



Scheme 2



Scheme 3



minima. To further refine the energies obtained from the B3LYP/BS1 calculations, we carried out single-point energy calculations for all of the structures with a larger basis set (BS2) in dichloromethane using the CPCM solvation model<sup>12</sup> at the B3LYP and M06<sup>13</sup> levels. BS2 utilizes the quadruple- $\zeta$  valence def2-QZVP<sup>14</sup> basis set on Au, Pd, and Sn and the 6-311+G(2d,p) basis set on other atoms. We have used the potential and Gibbs free energies obtained from the M06/BS2//B3LYP/BS1 calculations in dichloromethane throughout the paper unless otherwise stated. Recent computational studies on organometallic

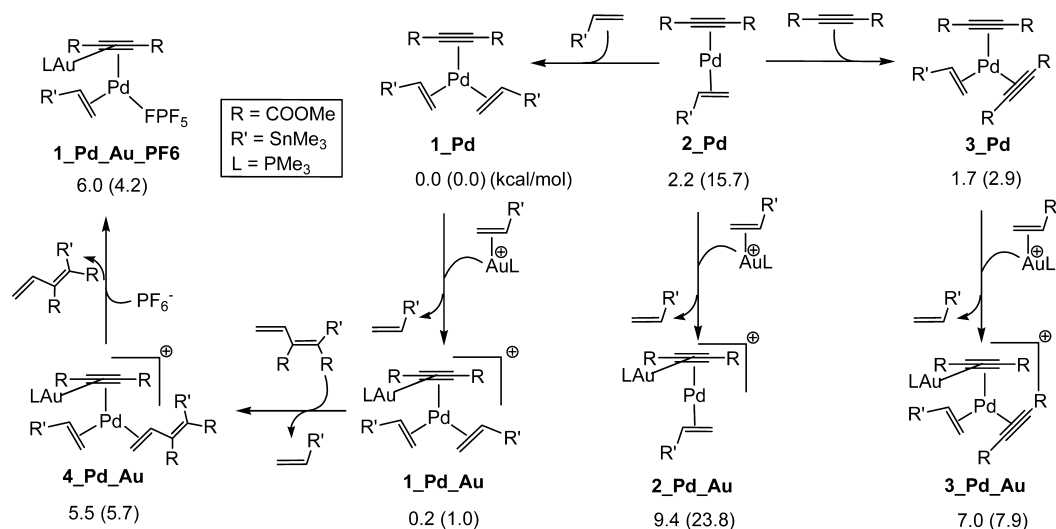
reactions have shown that thermodynamic and kinetic results are predicted more accurately if the M06 functional is used instead of B3LYP.<sup>13</sup> The use of M06 can also be rationalized based on the fact that this functional estimates the van der Waals interactions more precisely.<sup>15</sup> These factors have prompted us to select this functional for all the single point calculations. The atomic orbital populations were calculated on the basis of natural bond orbital (NBO) analyses.<sup>16</sup> In the calculations, SnBu<sub>3</sub> is simplified to SnMe<sub>3</sub>, and PMe<sub>3</sub> is used as the coordinated ligand to Au(I).

## RESULTS AND DISCUSSION

As discussed above, a combination of Pd<sub>2</sub>(dba)<sub>3</sub> and PPh<sub>3</sub>AuPF<sub>6</sub> is capable of catalyzing the vinylstannylation of alkynes, although no reaction is observed if only Pd<sub>2</sub>(dba)<sub>3</sub> is used as the catalyst. In view of these interesting findings, we are prompted first to address the question of why Pd<sub>2</sub>(dba)<sub>3</sub> is not able to catalyze the reaction. The main objective in addressing this issue is to find out what step is the most energy consuming, thus preventing the vinylstannylation reaction, and how the addition of LAu<sup>+</sup> avoids the energy consuming step by changing the reaction mechanism.

As dba is a weak coordinating ligand with a low concentration, the vinylstannylation reaction would likely be initiated through formation of three precursor complexes **1\_Pd**, **2\_Pd**, and/or **3\_Pd** (Scheme 4). Among these precursor complexes, **1\_Pd** is the most stable.<sup>17</sup> We only consider in the text the precursor complexes having both the vinylstannane and dimethyl acetylenedicarboxylate (DMAD) substrates coordinated to palladium. Other conceivable adducts either are less stable or have a comparable stability to **1\_Pd** (Scheme S1, Supporting Information). Figure 1 shows the free energy profile for the vinylstannylation reaction catalyzed by Pd<sup>0</sup> starting from **1\_Pd**. Analogous to Scheme 1 omitting gold, the reaction is surmised to proceed via oxidative addition of one of the Sn–C bonds to Pd<sup>0</sup>, followed by the alkyne insertion into the Pd–Sn bond, giving **4\_Pd**. These two steps are found to occur in one step.

Scheme 4



The Sn transfer reaction (formation of **4\_Pd**) is calculated to be very endergonic (24.3 kcal/mol). The resulting endergonicity may be attributed to the fact that two strong trans-influencing vinyl ligands are present as trans in **4\_Pd**. Intermediate **4\_Pd** then undergoes isomerization through transition structure **2TS\_Pd** to give the more stable intermediate **5\_Pd** in which the two vinyl ligands are cis to each other. From **5\_Pd**, the final product is formed through vinyl–vinyl reductive elimination. The isomerization reaction with an overall activation barrier as high as 38.6 kcal/mol is calculated to be the rate-determining step in the catalytic cycle. It follows from these results that Pd<sup>0</sup> alone is not capable of catalyzing the vinylstannylation reaction,

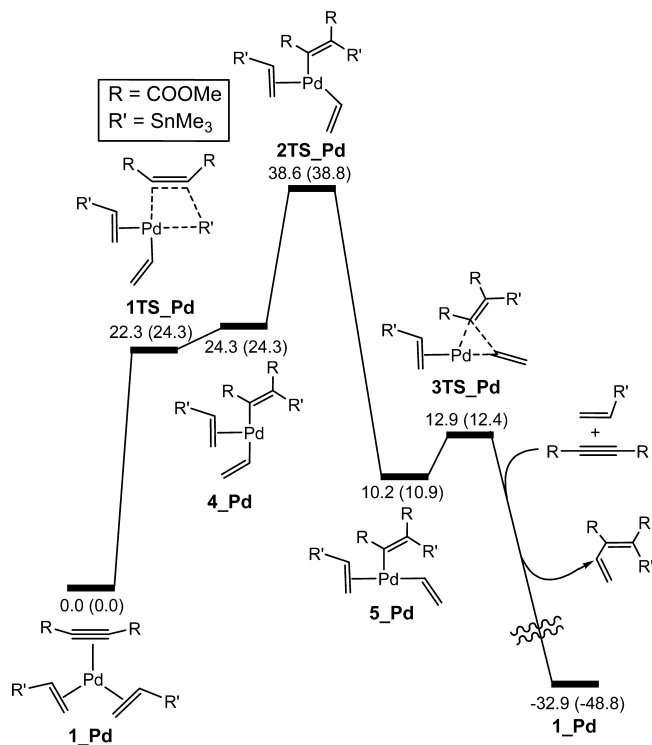


**Figure 1.** Energy profile calculated for carbostannylation of DMAD catalyzed by Pd<sup>0</sup> alone. The relative Gibbs and electronic energies (in parentheses) obtained from the M06/BS2//B3LYP/BS1 calculations in CH<sub>2</sub>Cl<sub>2</sub> are given in kcal/mol.

because the initial intermediate obtained from the Sn-to-Pd transmetalation reaction (**4\_Pd**) is highly unstable, and isomerization of this unstable intermediate (via Y-shaped transition structure **2TS\_Pd**) to an intermediate from which the C–C reductive elimination can occur is the most energy consuming process.<sup>18</sup>

We now turn our attention to the question of why the reaction is easily cocatalyzed by addition of PPh<sub>3</sub>AuPF<sub>6</sub>. It is anticipated that this addition can initially lead to the formation of various adducts, as shown with a few representative examples in Scheme 5.<sup>19</sup> Because **1\_Au** is calculated to be the most stable adduct, we consider this structure as the resting state for the gold precursor. According to Blum's mechanism depicted in Scheme 2, the reaction is proposed to start from an adduct in which both gold and palladium are simultaneously coordinated to alkyne. A few representative examples of these adducts are depicted in Scheme 4. Among these intermediates, **1\_Pd\_Au** is found to be the most stable, and thus we continue our investigation of the vinylstannylation reaction from this intermediate.<sup>20</sup>

As alkynes have two mutually perpendicular sets of  $\pi$  orbitals, we expect that one of them interacts with palladium and the other with gold. To this end, we found that in all possible intermediates, the C1–Pd–C2 plane is perpendicular to the C1–Au–C2 plane (for an example see **1\_Pd\_Au** in Figure 2). The coordination of Lewis acid [AuPMe<sub>3</sub>]<sup>+</sup> to the alkyne ligands causes the CO<sub>2</sub>Me substituents to fold back further

**Scheme 5**

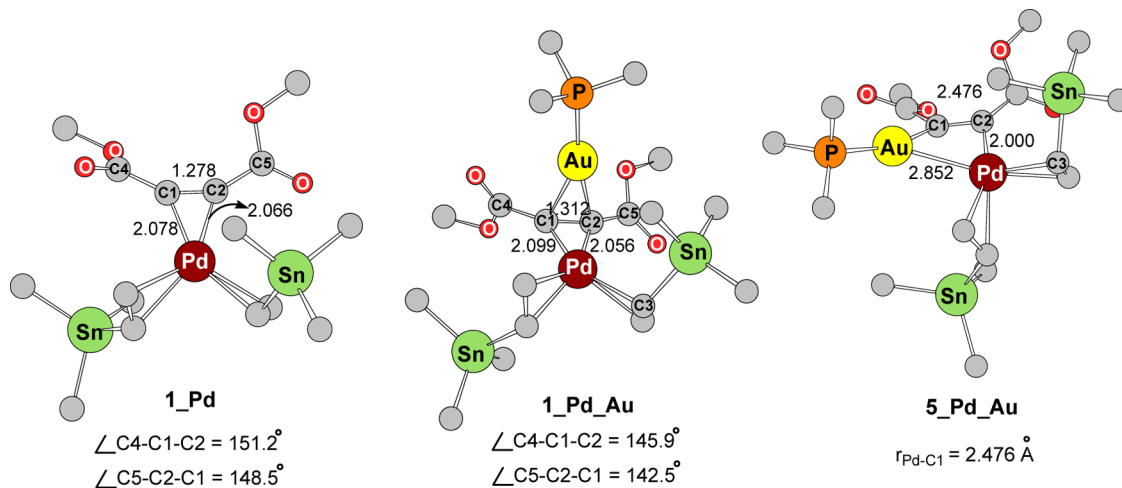
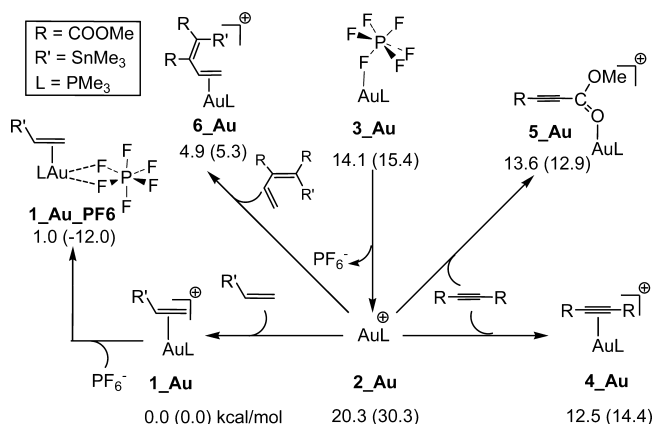


**Figure 2.** Optimized structures with selected structural parameters (bond lengths in angstroms) for **1\_Pd**, **1\_Pd\_Au**, and **5\_Pd\_Au** (H atoms omitted for clarity).

away from the metal and the C1–C2 bond distance to be lengthened, suggesting that the Au<sup>+</sup> coordination increases the palladium-to-alkyne back-donation, as proposed by Blum and co-workers.<sup>4</sup> However, this coordination does not affect significantly the Pd–C1 and Pd–C2 bond distances, a result which can be likely explained through a molecular orbital analysis. The coordination of [AuPMe<sub>3</sub>]<sup>+</sup> to the free alkyne reduces the energy of not only the C≡C π-antibonding orbitals but also the C≡C π-bonding orbitals (Figure 3). In such a case, the coordination is expected to shorten the Pd–C bonds due to the increased palladium-to-alkyne back-donation but this is nearly canceled out by the decreased alkyne-to-palladium donation.

Our calculations show that the intermediate **1\_Pd\_Au** is not able to undergo the Sn-to-Pd transmetalation reaction, and in order for the reaction to proceed further, this intermediate

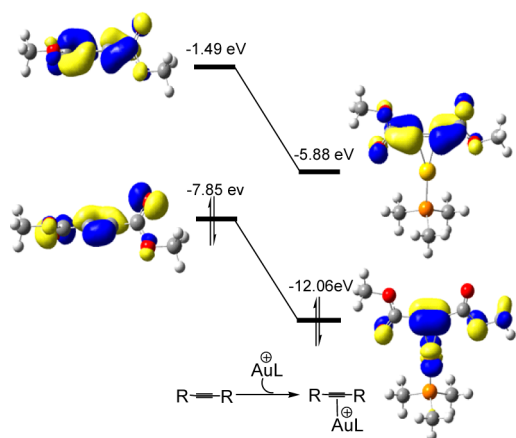


**Figure 3.** Spatial plots showing how the energies of the C≡C π-antibonding and π-bonding orbitals of DMAD change after coordination to Au<sup>I</sup>.

should isomerize to a palladium gold vinyl intermediate **5\_Pd\_Au** through the rotation of the Au–C1 bond around the Pd–C1 axis (Figures 2 and 4). This isomerization, which leads to oxidation of Pd<sup>0</sup> to Pd<sup>II</sup>, is found to be endergonic by 1.9 kcal/mol and only requires a low activation barrier (3.5 kcal/mol) relative to **1\_Pd\_Au**. The rotation results in two electrons being transferred from a Pd<sup>0</sup> d orbital to a C≡C π-antibonding orbital of alkyne through the C2 atom. Formally, palladium is oxidized to Pd<sup>II</sup>, and gold remains as Au<sup>I</sup>. Due to the oxidation of Pd<sup>0</sup> by two units, intermediate **5\_Pd\_Au** adopts a square planar geometry with a relatively weak Pd–Au interaction. The Pd–Au distance in **5\_Pd\_Au** (2.852 Å) (Figure 2) is shorter than the sum of the van der Waals radii of gold and palladium (3.290 Å). In addition, the Wiberg bond order between Au and Pd is calculated to be 0.254. The evolution of the Pd–Au distance for some of the species is shown in Figure 4.

We found that **1\_Au** can interact with **2\_Pd** through transition structure **5TS\_Pd\_Au** to give **9\_Pd\_Au** in which the gold(I) catalyst is bonded directly to the palladium(0) catalyst (Figure 5).<sup>21</sup> This type of coordination results in a charge transfer from Pd to Au and causes **9\_Pd\_Au** to undergo alkyne insertion into the Au–Pd bond with a low activation barrier of 3.7 kcal/mol to form **10\_Pd\_Au**. The coordination of a free vinylSnMe<sub>3</sub> substrate to **10\_Pd\_Au** gives the key intermediate **5\_Pd\_Au**. The result of the calculation suggests that the intermediates **5\_Pd\_Au** and **1\_Pd\_Au** can be in equilibrium prior to further progress from **5\_Pd\_Au** (Figure 5).

The next step from **5\_Pd\_Au** is surmised to be transmetalation from the vinyl–tin to vinyl–palladium (Figure 4), giving a tin gold vinyl complex coordinated to Pd<sup>II</sup> (intermediate **7\_Pd\_Au**). This process involves the oxidative addition of Me<sub>3</sub>Sn–C3 to Pd<sup>II</sup>, followed by Me<sub>3</sub>Sn–C2 reductive elimination.<sup>22</sup>

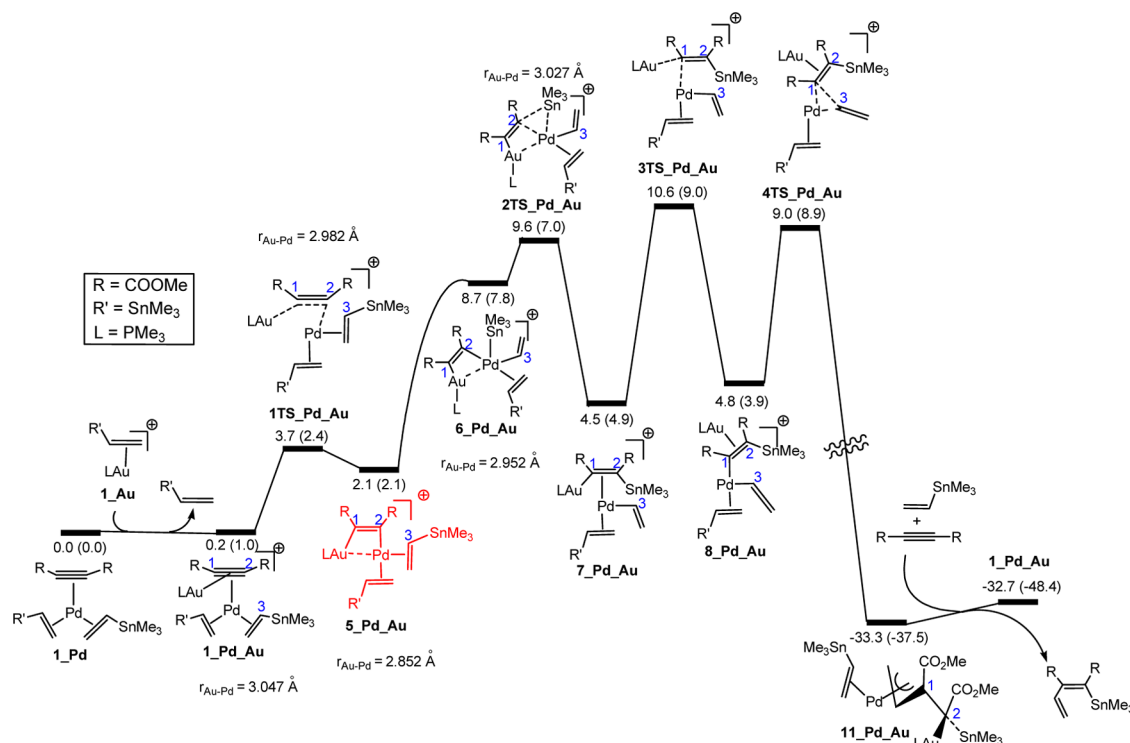


**Figure 4.** Energy profile calculated for carbostannylation of DMAD catalyzed by Pd<sup>0</sup>/Au<sup>I</sup> based on the catalytic cycle given in Scheme 6. The relative Gibbs and electronic energies (in parentheses) obtained from the M06/BS2//B3LYP/BS1 calculations in CH<sub>2</sub>Cl<sub>2</sub> are given in kcal/mol.



The oxidative addition step, which gives the palladium(IV) intermediate **6\_Pd\_Au**, is calculated to be almost barrierless<sup>23</sup> with a reaction free energy requirement of 6.6 kcal/mol. Compound **6\_Pd\_Au** then undergoes reductive elimination with a small barrier (0.9 kcal/mol) to afford **7\_Pd\_Au** (the product of transmetalation). The reaction free energy for formation of **7\_Pd\_Au** from **1\_Pd** is calculated as 4.5 kcal/mol, indicating that the product of the transmetalation step in the

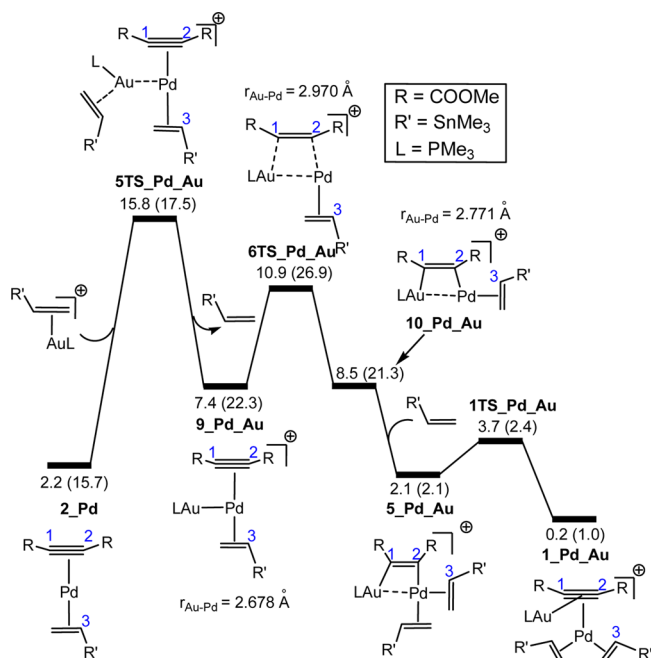


**Figure 5.** Energy profile showing equilibrium between four intermediates **9\_Pd\_Au**, **10\_Pd-Au**, **5\_Pd\_Au**, and **1\_Pd\_Au**. The relative Gibbs and electronic energies (in parentheses) obtained from the M06//BS2//B3LYP/BS1 calculations in CH<sub>2</sub>Cl<sub>2</sub> are given in kcal/mol.

bimetallic mechanism is about 19.8 kcal/mol more stable than that via the classical mechanism (intermediate **4\_Pd**) (Figures 1 and 4). The higher stability of **7\_Pd\_Au** can be attributed to the fact that the vinyl group transferred to palladium is trans to the vacant coordination site of Pd<sup>II</sup>, whereas the presence of two trans vinyl groups in **4\_Pd** (Figure 1) makes this compound very unstable. The Au-Pd bond distance in **6\_Pd\_Au** (2.952 Å) is longer than that in **5\_Pd\_Au**, most likely because of the stronger trans-influence property of the vinyl group compared to the alkene.

Our calculations provide evidence that the transmetalation can also occur through an alternative pathway in which the tin group initially migrates to the carbonyl group of the DMAD ligand and then to the C2 atom. This pathway at the M06 level (Figure 6) is calculated to be about 1 kcal/mol less favorable than that shown in Figure 1.

Starting from **7\_Pd\_Au** (Figure 4), the Au-to-Pd transmetalation<sup>24</sup> occurs through transfer of a vinyl group from Au to Pd to give intermediate **8\_Pd\_Au** in which Au<sup>I</sup> is coordinated to the π bond of the palladium's vinyl ligand. The reaction barrier for conversion of **7\_Pd\_Au** to **8\_Pd\_Au** is calculated to be 6.1 kcal/mol. This interesting result demonstrates that, in contrast to the Sn-to-Pd transmetalation,<sup>25</sup> the Au-to-Pd transmetalation can proceed without involvement of a non-innocent X ligand.<sup>26</sup> The vinyl-vinyl reductive elimination from **8\_Pd\_Au** with an activation barrier of 4.2 kcal/mol is calculated to lead to formation of the intermediate **11\_Pd\_Au** (vide infra) through which the product is formed via coordination of a vinylSnMe<sub>3</sub> to the empty site of **11\_Pd\_Au** followed by dissociation of the Au<sup>I</sup>-bound product (Figure S7, Supporting Information).

Scheme 6 shows the complete detailed catalytic cycle. It includes four major steps: (A) oxidation of Pd<sup>0</sup> to Pd<sup>II</sup> through formation of a palladium gold vinyl intermediate, (B) Sn-to-Pd transmetalation, (C) Au-to-Pd transmetalation, and (D) C-C reductive elimination. It follows from the calculations that the

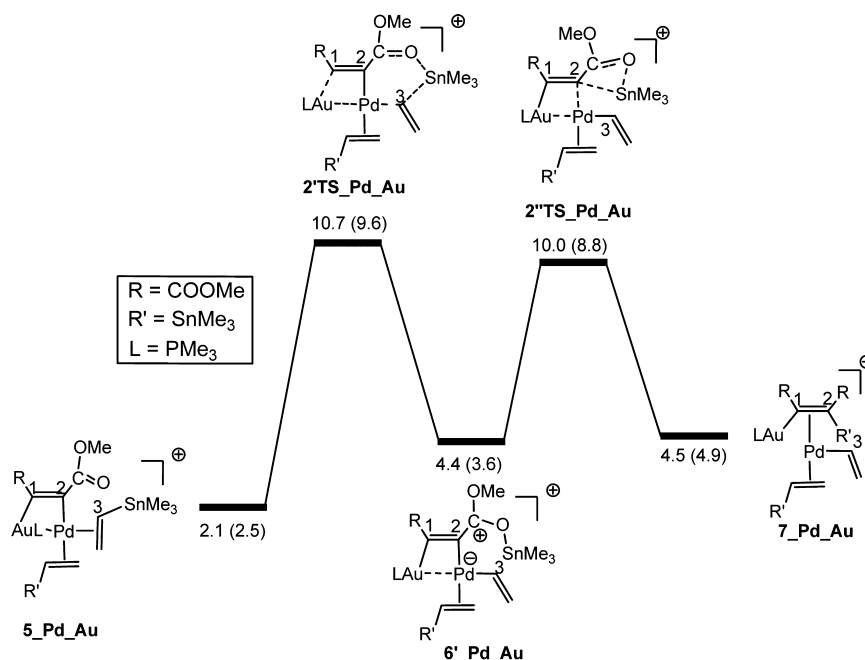
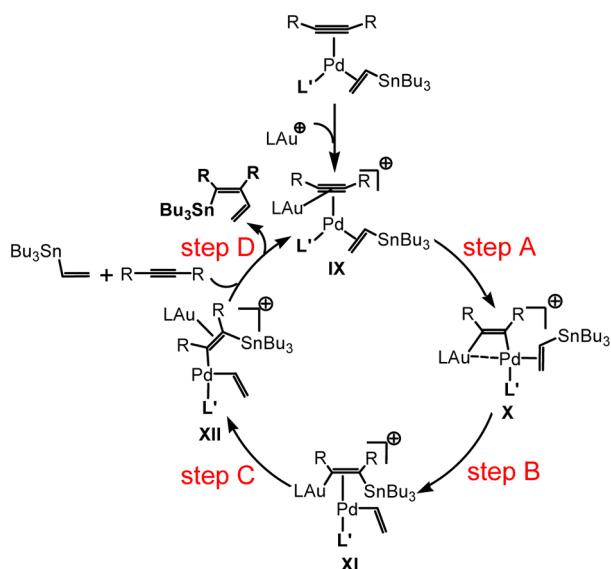


**Figure 6.** Energy profile showing an alternative pathway for Sn-to-Pd transmetalation in which the tin group migrates to the carbonyl group of the DMAD ligand and then to the C2 atom. The relative Gibbs and electronic energies (in parentheses) obtained from the M06/BS2//B3LYP/BS1 calculations in CH<sub>2</sub>Cl<sub>2</sub> are given in kcal/mol.

involvement of a  $\text{Au}^+$  complex reduces considerably the overall activation barrier of the vinylstannylation reaction. This reduction is from 38.6 kcal/mol in the classical mechanism (Figure 1) to 10.6 kcal/mol in the bimetallic mechanism (Figure 4)<sup>27</sup> if we ignore the process of formation of **1\_Pd\_Au**, which is calculated to be the most difficult step with a barrier of 15.8 kcal/mol (Figure 5). This reduction is mainly due to the fact that the intermediacy of palladium gold vinyl complex **5\_Pd\_Au** results in removal of the two energy consuming steps of the classical mechanism (i.e., the Sn-to-Pd transmetalation and isomerization steps), as depicted in Figure 1. The involvement of three formal oxidation states for palladium (0, II, IV) is also notable. In summary, our proposal involves determination that species **X** and **XI** are intermediates that occur between **I** and **II** in Blum's first proposal (Scheme 2).

**Proposed Mechanism for Formation of the Anti Addition Product.** Although the major product was found

Scheme 6



to be from syn addition, a small amount of the anti addition product was also reported by Blum and co-workers. Here, we are capable of accounting for the formation of the anti addition product through the following mechanism (Figure 7). As mentioned above, an IRC calculation from **4TS\_Pd\_Au** indicates that this transition structure connects to intermediate **11\_Pd\_Au** prior to the formation of the syn addition product. In this intermediate, the  $\pi$  bond between C1 and C2 of the final product is mainly polarized toward C2 due to the presence of the  $\text{Au}^I$  and  $\text{Pd}^0$  metals. Indeed, the Lewis acidity of  $\text{Au}^I$  induces the polarization of the  $\pi$  bond toward C2, resulting in the oxidation of  $\text{Pd}^0$  to  $\text{Pd}^{II}$  following the interaction of a Pd-occupied  $d_{\pi}$  orbital with the electron-deficient C1 atom, resulting in the formation of the  $\eta^3$ -allyl intermediate **11\_Pd\_Au**. In this intermediate, the nature of the C1–C2 bond mostly changes to  $\sigma$  character and thus this bond can easily undergo the rotation about the C1–C2 bond by passing intermediate **12\_Pd\_Au** to give an intermediate (**13\_Pd\_Au**) through which the anti addition product is formed. A plausible reason for why the anti addition is the minor product may be attributed to the lower stability of **13\_Pd\_Au** compared to **11\_Pd\_Au** (see Supporting Information for more details).

**Alternative Mechanism.** We also studied the alternative mechanism proposed by Blum and co-workers as outlined in Scheme 3. Given that the palladium precatalyst used by Blum and co-workers is  $\text{Pd}^0$ , it is not clear how the  $\text{Pd}^{II}$  intermediate **IV** is initially generated. We believe that the active catalyst should again be intermediate **X** (Scheme 6). This intermediate, with an oxidation state of +2 for palladium, can be used as the active catalyst for the catalytic cycle proposed by Blum and co-workers, rather than **V** in Scheme 3. In such a case, we have altered the corresponding catalytic cycle to that depicted in Scheme 7. We have considered the two key steps B and C of the alternative catalytic cycle for two different counterions  $X' = \text{PF}_6$  and  $\text{CF}_3\text{SO}_3$  (triflate) in Figures 8 and 9. According to the mechanism we envisage, the substitution reaction between **7\_Au** and **5\_Pd\_Au** gives **14\_Pd\_Au** and  $\text{vinylSnMe}_3$ . This reaction is calculated to be exergonic by about 4.9 kcal/mol, a result which might be attributed to the less-sterically hindered nature of  $\text{AuPMe}_3$  as compared to  $\text{SnMe}_3$ . Once **14\_Pd\_Au** is

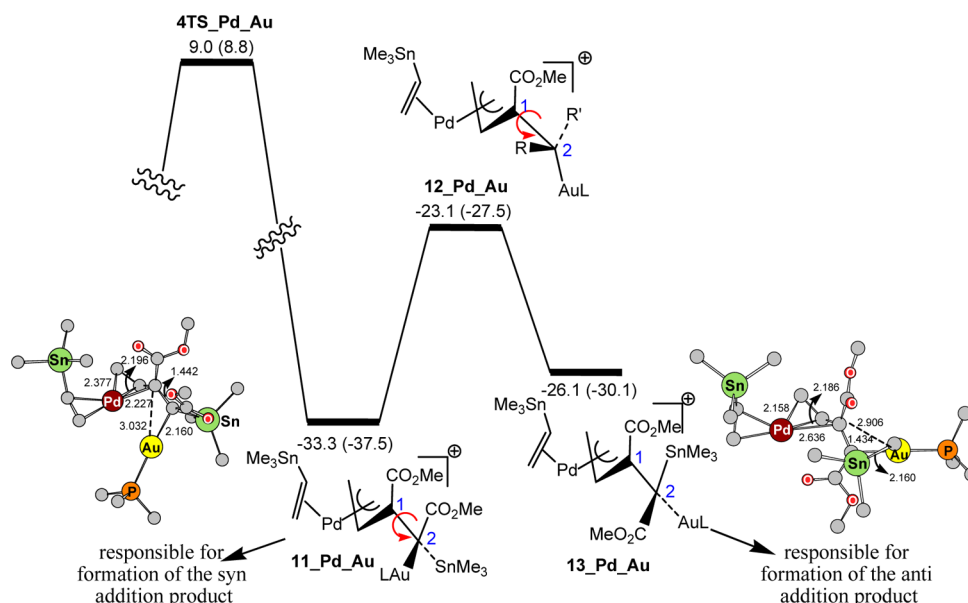


**Figure 7.** Energy profile showing interconversion between the intermediates responsible for the syn and anti addition products. The relative Gibbs and electronic energies (in parentheses) obtained from the M06/BS2//B3LYP/BS1 calculations in  $\text{CH}_2\text{Cl}_2$  are given in kcal/mol.

Scheme 7

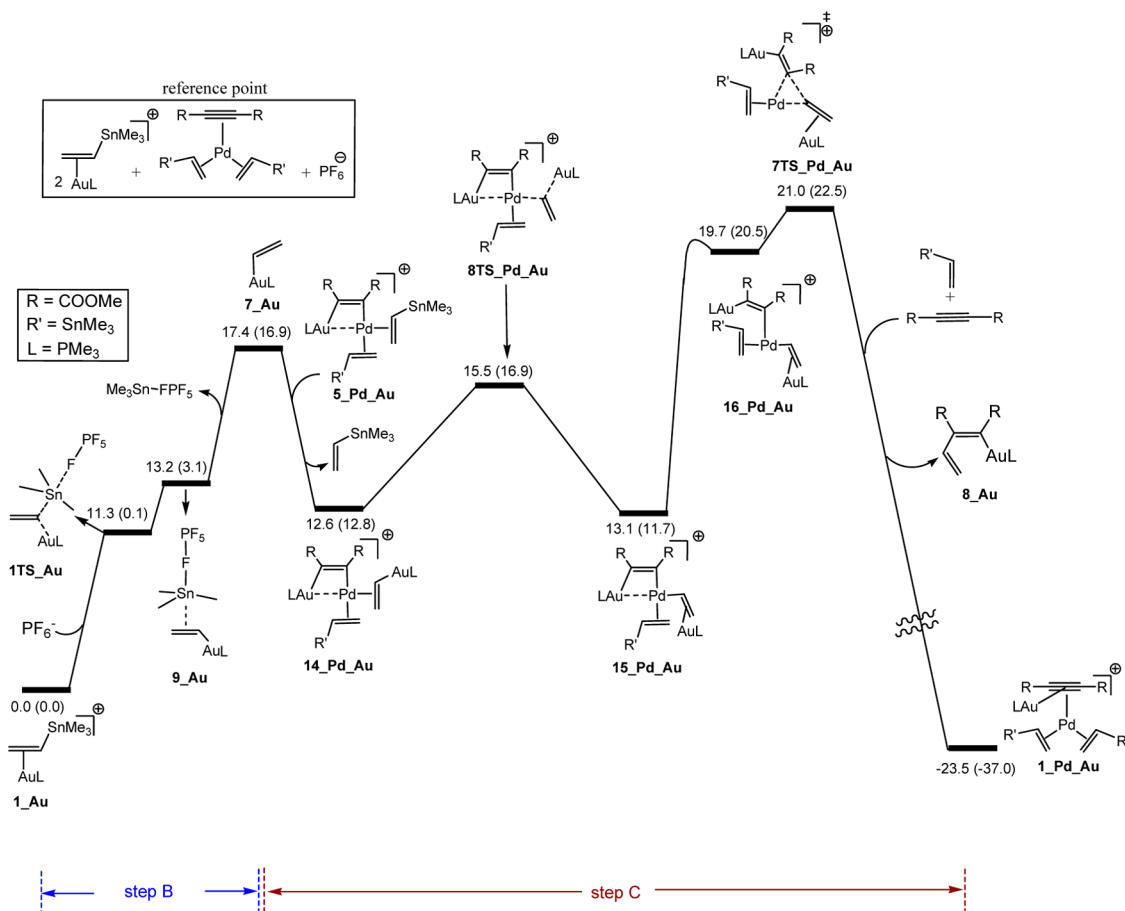
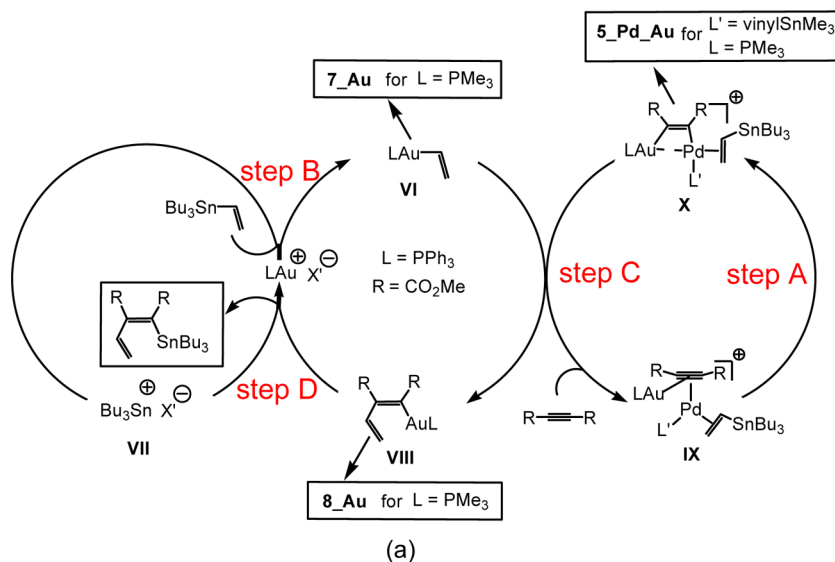


**Figure 8.** Energy profile calculated for steps B and C of the catalytic cycle given in Scheme 7 in the presence of  $\text{PF}_6^-$  counteranion. The relative Gibbs and electronic energies (in parentheses) obtained from the M06/BS2//B3LYP/BS1 calculations in  $\text{CH}_2\text{Cl}_2$  are given in kcal/mol.

formed, the reaction further progresses through Au-to-Pd transmetalation to give **15\_Pd\_Au**, followed by the isomerization to **16\_Pd\_Au**<sup>23</sup> and then the vinyl–vinyl reductive elimination through transition structure **7TS\_Pd\_Au**.

It is found that, regardless of the identity of  $\text{X}'$ , the Sn-to-Au transmetalation (formation of **7\_Au**) occurs almost without any significant activation barrier (Figures 8 and 9). This finding

explains why the reaction of  $\text{LAu}(\text{triflate}) + \text{Bu}_3\text{Sn}(\text{vinyl}) \rightarrow \text{LAu}(\text{vinyl}) + \text{Bu}_3\text{Sn}(\text{triflate})$ , as discovered by Blum and co-workers,<sup>2b</sup> is immediately complete.

Interestingly, we found that the overall activation barrier of the C–C reductive elimination mainly depends on the identity of the counterion  $\text{X}'$ . If  $\text{X}' = \text{PF}_6^-$  (Figure 8), the counterion used experimentally (Scheme 1), the relative Gibbs energy of

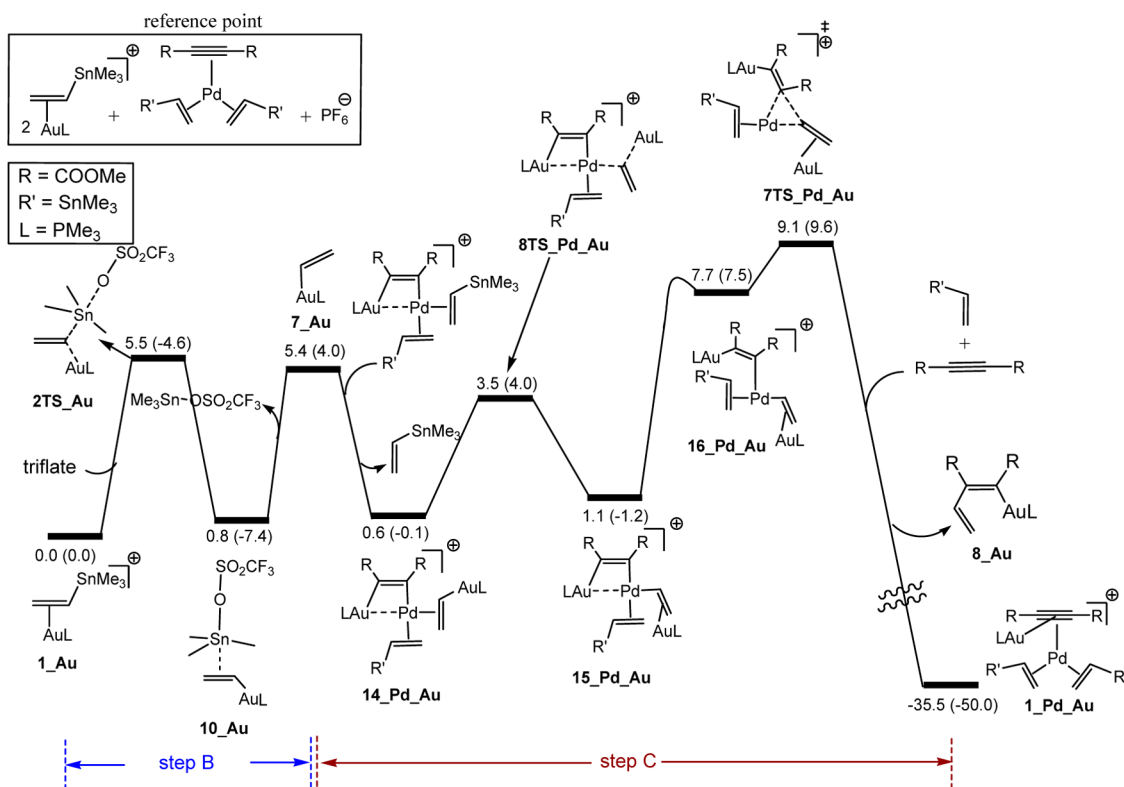


**Figure 9.** Energy profile calculated for steps B and C of the catalytic cycle given in Scheme 7 in the presence of the  $\text{CF}_3\text{SO}_3^-$  counteranion. The relative Gibbs and electronic energies (in parentheses) obtained from the M06/BS2//B3LYP/BS1 calculations in  $\text{CH}_2\text{Cl}_2$  are given in kcal/mol.

$7\text{TS}_{\text{Pd}_{\text{Au}}}$  is calculated to be 21.0 kcal/mol. This result indicates that  $7\text{TS}_{\text{Pd}_{\text{Au}}}$  lies above transition structures  $2\text{TS}_{\text{Pd}_{\text{Au}}}$ ,  $3\text{TS}_{\text{Pd}_{\text{Au}}}$ , and  $4\text{TS}_{\text{Pd}_{\text{Au}}}$  (Figure 4), suggesting that the mechanism given in Scheme 7 is less likely to be operative. In contrast, if  $\text{X}' = \text{CF}_3\text{SO}_3^-$  (Figure 9), the overall reaction barrier is calculated as 9.1 kcal/mol, suggesting that both mechanisms might be competitive.

The strong dependency of the alternative mechanism (Scheme 7) on the identity of  $\text{X}'$  is related to the fact that the thermodynamics of the Sn-to-Au transmetalation (step B) are intensively reliant on  $\text{X}'$ , a result which has been proved experimentally by Casares, Espinet, and co-workers, for example, in studies of the reaction of  $\text{R}_3\text{SnBu}_3$  ( $\text{R} = \text{aryl, alkynyl}$ ) with  $\text{PPh}_3\text{AuX}$  ( $\text{X} = \text{Cl, I}$ ).<sup>28</sup> In the present case, the Gibbs reaction energy of  $1_{\text{Au}} + \text{X}'^- \rightarrow \text{Me}_3\text{SnX}' + 7_{\text{Au}}$  is computed as 17.4 and 5.4 kcal/mol for  $\text{X}' = \text{PF}_6^-$  (Figure 6) and  $\text{CF}_3\text{SO}_3^-$  (Figure 7), respectively. Because  $\text{PF}_6^-$  is used as the counterion in the experiment,<sup>4</sup> the Sn-to-Au transmetalation is predicted to be extremely endergonic and therefore the alternative mechanism is not expected to be the favored mechanism.

## CONCLUSION

We have investigated computationally the gold and palladium cocatalyzed vinylstannylation of dimethyl acetylenedicarboxylate (DMAD).<sup>29</sup> In conclusion, the computational study confirms the role of intermediates containing both palladium and gold in a mechanism proposed by Blum (Scheme 2), with the additional involvement of **X** and **XI** as shown in Scheme 6. Species **X** and **XI** occur between **I** and **II** in Blum's original proposal. We find also the requirement for a Pd(IV) intermediate ( $6_{\text{Pd}_{\text{Au}}}$  in Figure 4), on the pathway between **X** and **XI**. Our work also

gives extensive support for Blum's second mechanism (Scheme 3) and accounts for the effect of the anion in the conditions where this mechanism is preferred over the first proposal. Computation indicates that this mechanism should now also include species containing both palladium and gold, **IX** and **X** in place of **IV** and **V**, respectively, in Scheme 3, as illustrated in the revised mechanism (Scheme 7). Particularly notable is the key role of **X** in both mechanisms, where **X** is a palladium gold vinyl intermediate which has an aurophilic interaction between Pd and Au with formal oxidation states Au(I) and Pd(II).

## ASSOCIATED CONTENT

### Supporting Information

Text giving the complete ref 6, a table giving Cartesian coordinates of all optimized structures along with energies, figures giving the calculated energy profiles obtained by the B3LYP level, a plausible mechanism for the formation of  $1_{\text{Pd}}$  from  $\text{Pd}_2(\text{dba})_3$ , an energy profile that compares the reactivity of other intermediates with  $1_{\text{Pd}_{\text{Au}}}$ , a figure giving the scanned PES between  $5_{\text{Pd}_{\text{Au}}}$  and  $6_{\text{Pd}_{\text{Au}}}$ , the optimized structures of the intermediates and the transition structures, a conceivable mechanism for releasing the final product from the vinyl complexes  $11_{\text{Pd}_{\text{Au}}}$  and  $13_{\text{Pd}_{\text{Au}}}$ , and a plausible explanation for slow addition of alkyne. This material is available free of charge via the Internet at <http://pubs.acs.org>.

## AUTHOR INFORMATION

### Corresponding Authors

\*E-mail: [ariafard@yahoo.com](mailto:ariafard@yahoo.com) (A.A.).

\*E-mail: [Brian.Yates@utas.edu.au](mailto:Brian.Yates@utas.edu.au) (B.F.Y.).

### Notes

The authors declare no competing financial interest.



## ACKNOWLEDGMENTS

We thank the Australian Research Council for financial support and the Australian National Computational Infrastructure and the University of Tasmania for computing resources. A.A., N.A.R., and M.J.A. are grateful for the financial support of the Islamic Azad University, Central Tehran Branch.

## REFERENCES

- (1) For recent examples of bimetallic catalysts, see (a) Shi, Y.; Roth, K. E.; Ramgren, S. D.; Blum, S. A. *J. Am. Chem. Soc.* **2009**, *131*, 18022. (b) Chuang, G. J.; Wang, W.; Lee, E.; Ritter, T. *J. Am. Chem. Soc.* **2011**, *133*, 1760. (c) Johnson, S. A.; Beck, R. *Chem. Commun.* **2011**, 47, 9233. (d) Gu, Z.; Herrmann, A. T.; Zakarian, A. *Angew. Chem., Int. Ed.* **2011**, *50*, 7136. (e) Trost, B. M.; Luan, X.; Miller, Y. *J. Am. Chem. Soc.* **2011**, *133*, 12824. (f) Wang, Y.-F.; Toh, K. K.; Lee, J. Y.; Chiba, S. *Angew. Chem., Int. Ed.* **2011**, *50*, 5927. (g) Powers, D. C.; Lee, E.; Ariafard, A.; Sanford, M. S.; Yates, B. F.; Canty, A. J.; Ritter, T. *J. Am. Chem. Soc.* **2012**, *134*, 12002. (h) Hirner, J. J.; Roth, K. E.; Shi, Y.; Blum, S. A. *Organometallics* **2012**, *31*, 6843. (i) Ghorbani, N.; Mahdizadeh Ghohe, N.; Torabi, S.; Yates, B. F.; Ariafard, A. *Organometallics* **2013**, *32*, 1687. (j) Canty, A. J.; Ariafard, A.; Sanford, M. S.; Yates, B. F. *Organometallics* **2013**, *32*, 544. (k) Mustard, T. J. L.; Mack, D. J.; Njardarson, J. T.; Cheong, P. H.-Y. *J. Am. Chem. Soc.* **2013**, *135*, 1471.
- (2) For reviews, see (a) Van den Beuken, E. K.; Feringa, B. L. *Tetrahedron* **1998**, *54*, 12985. (b) Hirner, J. J.; Shi, Y.; Blum, S. A. *Acc. Chem. Res.* **2011**, *44*, 603. (c) Pérez-Temprano, M. H.; Casares, J. A.; Espinet, P. *Chem.—Eur. J.* **2012**, *18*, 1864. (d) Powers, D. C.; Ritter, T. *Acc. Chem. Res.* **2012**, *45*, 840.
- (3) Attempts for the carbostannylation of alkynes catalysed by only Pd<sup>0</sup> have led to the double-addition products. (a) Shirakawa, E.; Yoshida, H.; Nakao, Y.; Hiyama, T. *J. Am. Chem. Soc.* **1999**, *121*, 4290. (b) Yoshida, H.; Shirakawa, E.; Nakao, Y.; Honda, Y.; Hiyama, T. *Bull. Chem. Soc. Jpn.* **2001**, *74*, 637.
- (4) Shi, Y.; Peterson, S. M.; Haberaecker, W. W., III; Blum, S. A. *J. Am. Chem. Soc.* **2008**, *130*, 2168.
- (5) Duschek, A.; Kirsch, S. F. *Angew. Chem., Int. Ed.* **2008**, *47*, 5703.
- (6) Frisch, M. J.; Trucks, G. W.; Schlegel, H. B.; Scuseria, G. E.; Robb, M. A.; Cheeseman, J. R.; Scalmani, G.; Barone, V.; Mennucci, B.; Petersson, G. A.; Nakatsuji, H.; Caricato, M.; Li, X.; Hratchian, H. P.; Izmaylov, A. F.; Bloino, J.; Zheng, G.; Sonnenberg, J. L.; Hada, M.; Ehara, M.; Toyota, K.; Fukuda, R.; Hasegawa, J.; Ishida, M.; Nakajima, T.; Honda, Y.; Kitao, O.; Nakai, H.; Vreven, T.; Montgomery, J. A.; Peralta, Jr., J. E.; Ogliaro, F.; Bearpark, M.; Heyd, J. J.; Brothers, E.; Kudin, K. N.; Staroverov, V. N.; Kobayashi, R.; Normand, J.; Raghavachari, K.; Rendell, A.; Burant, J. C.; Iyengar, S. S.; Tomasi, J.; Cossi, M.; Rega, N.; Millam, J. M.; Klene, M.; Knox, J. E.; Cross, J. B.; Bakken, V.; Adamo, C.; Jaramillo, J.; Gomperts, R.; Stratmann, R. E.; Yazyev, O.; Austin, A. J.; Cammi, R.; Pomelli, C.; Ochterski, J. W.; Martin, R. L.; Morokuma, K.; Zakrzewski, V. G.; Voth, G. A.; Salvador, P.; Dannenberg, J. J.; Dapprich, S.; Daniels, A. D.; Farkas, O.; Foresman, J. B.; Ortiz, J. V.; Cioslowski, J.; Fox, D. J. *Gaussian 09*, revision A.02; Gaussian, Inc.: Wallingford, CT, 2009.
- (7) (a) Lee, C. T.; Yang, W. T.; Parr, R. G. *Phys. Rev. B.* **1988**, *37*, 785. (b) Miehlisch, B.; Savin, A.; Stoll, H.; Preuss, H. *Chem. Phys. Lett.* **1989**, *157*, 200. (c) Becke, A. D. *J. Chem. Phys.* **1993**, *98*, 5648.
- (8) (a) Hay, P. J.; Wadt, W. R. *J. Chem. Phys.* **1985**, *82*, 270. (b) Wadt, W. R.; Hay, P. J. *J. Chem. Phys.* **1985**, *82*, 284.
- (9) Hariharan, P. C.; Pople, J. A. *Theor. Chim. Acta* **1973**, *28*, 213.
- (10) (a) Ehlers, A. W.; Böhme, M.; Dapprich, S.; Gobbi, A.; Höllwarth, A.; Jonas, V.; Köhler, K. F.; Stegmann, R.; Veldkamp, A.; Frenking, G. *Chem. Phys. Lett.* **1993**, *208*, 111. (b) Höllwarth, A.; Böhme, M.; Dapprich, S.; Ehlers, A. W.; Gobbi, A.; Jonas, V.; Köhler, K. F.; Stegmann, R.; Veldkamp, A.; Frenking, G. *Chem. Phys. Lett.* **1993**, *208*, 237.
- (11) (a) Fukui, K. *J. Phys. Chem.* **1970**, *74*, 4161. (b) Fukui, K. *Acc. Chem. Res.* **1981**, *14*, 363.
- (12) Barone, V.; Cossi, M. *J. Phys. Chem. A.* **1998**, *102*, 1995.
- (13) Zhao, Y.; Truhlar, D. G. *Acc. Chem. Res.* **2008**, *41*, 157.
- (14) Weigend, F.; Furche, F.; Ahlrichs, R. *J. Chem. Phys.* **2003**, *119*, 12753.
- (15) Sieffert, N.; Bühl, M. *Inorg. Chem.* **2009**, *48*, 4622.
- (16) Glendening, E. D.; Read, A. E.; Carpenter, J. E.; Weinhold, F. *NBO*, version 3.1; Gaussian, Inc.: Pittsburgh, PA, 2003.
- (17) A plausible mechanism for the formation of **1\_Pd** starting from Pd<sub>2</sub>(dba)<sub>3</sub> is delineated in Figure S1. This reaction is predicted to be a kinetically easy process with a reaction free energy of  $-1.2$  kcal/mol.
- (18) In such Y-shaped transition structures, the occupied d<sub>xy</sub> orbital of palladium is destabilized due to the overlap with the migrating group in an antibonding fashion. Because the migrating group in **2TS\_Pd** is a vinyl group with a strong trans influence property, the Pd d<sub>xy</sub> orbital is considerably destabilized, thereby resulting in a significant instability of the transition structure **2TS\_Pd** relative to **4\_Pd**. For more details, see Albright, T. A.; Burdett, J. K.; Whangbo, M.-H. *Orbital Interactions in Chemistry*; Wiley: New York, 1985; p 341.
- (19) The formation of a three coordinate Au complex through binding of PF<sub>6</sub><sup>-</sup> to **1\_Au** is an unfavorable process and leads to the ion pair **1\_Au-PF6** (Scheme 5). The optimized structure can still be described as a linear gold complex due to the d<sup>10</sup> configuration of the gold metal centre.
- (20) We have also investigated the vinylstannylation reaction starting from other possible intermediates and found that they are much less reactive than **1\_Pd\_Au** (Figure S4, Supporting Information). For example, the reductive elimination transition structures starting from catalyst precursors **2\_Pd\_Au**, **3\_Pd\_Au**, **1\_Pd\_Au-PF6** are calculated to be 9.2, 8.1, and 11.8 kcal/mol, respectively, higher in energy than **4TS\_Pd\_Au**.
- (21) All attempts to optimize a structure in which the LAu<sup>+</sup> catalyst is directly bonded to the Pd metal center of **1\_Pd\_Au** were not successful and led to the formation of **5\_Pd\_Au**.
- (22) Attempts to locate a four-centered transition structure through which **5\_Pd\_Au** is directly transformed into **7\_Pd\_Au** were unsuccessful and led to the transition structure **2TS\_Pd\_Au**.
- (23) We are not capable of locating the transition structures connecting **5\_Pd\_Au** to **6\_Pd\_Au** (Figure 4) and **15\_Pd\_Au** to **16\_Pd\_Au** (Figures 8 and 9) due to the flatness of the potential energy surface (PES) near the transition structures. In such a case, the reaction barriers are too small to be located. We scanned the PES between **5\_Pd\_Au** and **6\_Pd\_Au** (Figure S5) by optimizing geometries at various fixed values of the Sn-C3 distance followed by performing single point calculations for each point at the M06/BS2//B3LYP/BS2 level. Figure S5 confirms that the process **5\_Pd\_Au** → **6\_Pd\_Au** has a flat potential energy surface with a very small activation energy.
- (24) (a) Shi, Y.; Ramgren, S. D.; Blum, S. A. *Organometallics* **2009**, *28*, 1275. (b) Hashmi, A. S. K.; Lothschütz, C.; Döpp, R.; Rudolph, M.; Ramamurthi, T. D.; Rominger, F. *Angew. Chem., Int. Ed.* **2009**, *48*, 8243. (c) Hashmi, A. S. K.; Döpp, R.; Lothschütz, C.; Rudolph, M.; Riedel, D.; Rominger, F. *Adv. Synth. Catal.* **2010**, *352*, 1307. (d) Pérez-Temprano, M.; Casares, J. A.; de Lera, A. R.; Álvarez, R.; Espinet, P. *Angew. Chem., Int. Ed.* **2012**, *51*, 4917.
- (25) (a) Ariafard, A.; Lin, Z.; Fairlamb, I. J. S. *Organometallics* **2006**, *25*, 5788. (b) Nova, A.; Ujaque, G.; Maseras, F.; Lledós, A.; Espinet, P. *J. Am. Chem. Soc.* **2006**, *128*, 14571. (c) Ariafard, A.; Yates, B. F. *J. Am. Chem. Soc.* **2009**, *131*, 13981.
- (26) For another example in which the Au-to-Pd transmetalation proceeds without involvement of a non-innocent ligand, see Pérez-Temprano, M. H.; Casares, J. A.; de Lera, A. R.; Álvarez, R.; Espinet, P. *Angew. Chem., Int. Ed.* **2012**, *124*, 5001.
- (27) In agreement with the M06/BS2//B3LYP/BS1 functional, B3LYP/BS2//B3LYP/BS1 shows that the overall activation barrier of the vinylstannylation reaction is reduced from 37.0 kcal/mol in the classical mechanism (Figure S2) to 15.2 kcal/mol in the bimetallic mechanism (Figure S3).
- (28) delPozo, J.; Carrasco, D.; Pérez-Temprano, M. H.; García-Melchor, M.; Álvarez, R.; Casares, J. A.; Espinet, P. *Angew. Chem., Int. Ed.* **2013**, *52*, 2189.

(29) Blum and co-workers found that alkyne oligomerization is a competitive reaction for the vinylstannylation which can be avoided by slow addition of the alkyne (ref 4). We found that, starting from **3\_Pd\_Au**, the alkyne insertion into the Pd-C(vinyl) bond needs an activation energy comparable to that required for the vinylstannylation reaction from **1\_Pd\_Au** (see Supporting Information for more details).